A Thermal Image-based Fault Detection System for Solar Panels

Litty Koshy
Dept. of CSE,
SCMS School of Engineering and Technology
littykoshy@scmsgroup.org

Vaishnav M. V.
Dept. of CSE,
SCMS School of Engineering and Technology
vaishnavam02@gmail.com

Soumya Sunil
Dept. of CSE,
SCMS School of Engineering and Technology
soumyasunil3007@gmail.com

Savio Vinu Abraham
Dept. of CSE,
SCMS School of Engineering and Technology
saviovinuabr@gmail.com

Shivang Vidhyadharan
Dept. of CSE,
SCMS School of Engineering and Technology
shivangv2000@gmail.com

2024 International Conference on Cybernation and Computation (CYBERCOM) | 979-8-3315-4234-4/24/$31.00 ©2024 IEEE | DOI: 10.1109/CYBERCOM63683.2024.10803145

Abstract – The proliferation of solar photovoltaic (PV) systems necessitates efficient strategies for inspecting and classifying anomalies in endoflife modules, which contain heavy metals posing environ- mental risks. In this paper, we propose a comprehensive approach integrating infrared (IR) imaging and deep learning techniques, including ResNet and custom CNNs. Our methodology utilizes IR cameras to remotely capture temperature distributions on solar modules, leveraging Res-Net and custom CNNs for accurate anomaly detection and classification. Additionally, deblurring and SRR techniques are introduced to enhance the quality of IR images, thereby improving the performance of anomaly detection. We validate our model using a dataset comprising pictures taken from an IR camera in real solar farms, containing various anomaly types. The results were tested to demonstrate the effectiveness of our method. An average prediction accuracy of 94% was achieved and 12 parameters were classified with 86% accuracy. This research contributes to the optimization of solar energy systems by providing a reliable method for identifying and addressing anomalies, thereby enhancing their performance and environmental sustainability.

Index Terms—Solar photovoltaic modules, ResNet 50, Convolu- tional neural networks (CNNs),

I. INTRODUCTION

With the exponential growth of solar photovoltaic (PV) systems driven by advancements in nanomaterial technology, the global PV capacity has surged past 500 GW, experiencing a remarkable increase of 142 GW in 2020 alone, with the US contributing nearly 77 GW. Projections indicate that the Asia-Pacific region will dominate future installations, accounting for 55% of the global PV capacity over the next five years. This surge underscores the critical need for effective inspection and maintenance strategies, given the corresponding increase in end-of-life PV modules containing heavy metals and the environmental hazards they pose. Primarily fabricated using crystalline silicon (c-Si) technology or thin-film technology, PV modules are susceptible to various damages from environmental factors and mechanical stresses, which can curtail their life span and compromise their performance, ultimately leading to economic inefficiencies and environment pollution.

II. LITERTURE SURVEY

Efficient and non-destructive testing methods are imperative for the routine inspection of PV modules, with recent attention turning to remote sensing techniques such as electroluminescence (EL) imaging, infrared radiation (IR) imaging, and RGB imaging. While these methods offer rapid data acquisition, they often necessitate manual inspection and entail significant processing times. Acikgoz et al[1] employ a deep learning model specifically designed to classify hotspots in PV modules. Their approach focuses on using convolutional neural networks (CNNs) to capture the unique infrared patterns associated with these anomalies. They note the use of data augmentation techniques to mitigate issues like data imbalance, which can adversely affect classifier performance, particularly for minority classes. Their study also explores the challenges in reproducibility due to specific hardware and software dependencies. Le et al. [2] develop a deep CNN for remote anomaly detection in PV modules. Their approach emphasizes analyzing visual data to identify and classify faults such as hotspots and cracks. However, they discuss the operational challenges of implementing such systems, such as computational overhead, energy requirements, communication delays in remote monitoring, and the difficulty in integrating these systems with existing infrastructure. In[3],authors further expand on fault classification in PV modules by leveraging transfer learning and multi-scale CNNs. Their architecture benefits from transfer learning, which allows for quicker model convergence by utilizing pre-trained weights from large datasets. This method improves both the detection accuracy and processing efficiency. Tang et al. [4] apply deep learning to defect identification in PV modules using electroluminescence (EL) images. Their architecture focuses on enhancing the ability to detect and classify defects such as cracks, with automatic feature extraction using deep CNNs. This study emphasizes the importance of high-resolution EL images in improving the precision of defect identification.

Advances in deep learning, automatic detection of PV module damage have resulted from the application of various neural network (CNN) architectures, including LeNet, VGG, Fast RCCN, and U-net [6-10] and have been demonstrated with incredible accuracy of 75% to 100% in healthy separation. and bad photovoltaic cells. However, most existing methods primarily focus on indoor testing and small-scale defects, limiting their applicability to large-scale outdoor PV farms. To address these limitations, a deep learning-based method is used to analyze photovoltaic modules using infrared images, using one of the largest publicly available databases of 20,000 infrared images from real photovoltaic farms in six countries.

Our method employs a combination of pre-trained models, including ResNet-50 and custom convolutional neural

networks (CNNs), augmented by advanced techniques such as deblurring and super-resolution reconstruction (SRR), to increase the accuracy and efficiency of defect detection. We aim not only to efficiently classify different types of damages but also to mitigate the challenges posed by imbalanced datasets through effective offline augmentation methods. This paper represents the first comprehensive study utilizing such a large-scale IR image dataset for PV module inspection. Our contributions include the development of deep learning models to effectively detect and classify damaged PV devices, as well as techniques to deal with data inconsistencies. It is anticipated that this research will serve as a foundation for future studies and contribute to the development of non-destructive solutions for photovoltaic plants.

III. Classification Approach And Dataset

The construction method for PV module failure rating consists of several important steps, as shown in Figure 1. The data is then split into training, validation, and testing subsets. ResNet50 and CNN were used for comparison and metrics were derived from these models.

Fig. 1. Overview of classification approach used in this study

The InfraredSolarModules dataset, facilitated by Raptor Maps, fills a crucial role in machine learning research by offering a comprehensive collection of real-world infrared imagery from solar farms, showcasing various anomalies observed in photovoltaic installations. This dataset aims to support researchers in developing effective solutions to enhance the performance and sustainability of solar energy systems. Photovoltaic installations are susceptible to malfunctions, particularly concerning solar panels, due to the challenging operational conditions they face. Leveraging thermography, particularly through drones equipped with infrared cameras, emerges as a valuable preventive maintenance technique for identifying module abnormalities. This approach minimizes disruptions to energy generation processes within photovoltaic systems, highlighting the importance of data-driven strategies in optimizing solar energy output while mitigating environmental impact.

The dataset contains 20,000 infrared images, each with dimensions of 24 by 40 pixels. It includes 12 distinct categories of solar modules: 11 categories correspond to various anomalies, while one category represents the absence of anomalies (No-Anomaly). Initially, 80% of the images are allocated to the training set, with the remaining images evenly split between validation and testing sets. The reversing, filtering and sharpening processes are applied to images in the different classes. Table 1. shows the description of classes in the dataset.

An example of the data development process is shown in Figure 2.

To eliminate the imbalance in the dataset, data augmentation techniques were used. Figure 3. shows the data augmentation techniques which include operations such as rotations, flips, translations, brightness adjustments, and noise addition to improve the robustness of a model by increasing the variability in the training dataset without requiring additional data collection.

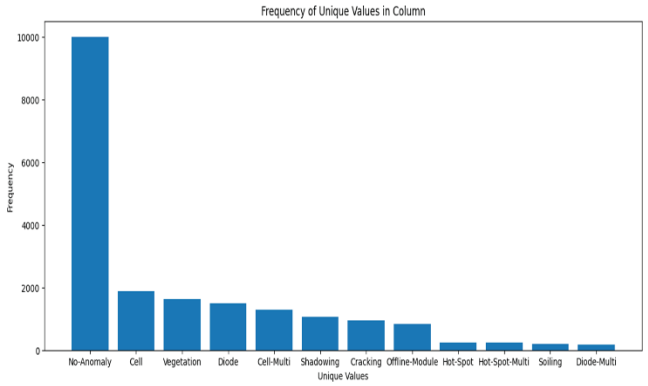

Fig. 2. Frequency of Unique Values in Column

When inverted, the hotspot image rotates 180° counterclockwise. Two-dimensional Gaussian filtering is used in the filtering process. A Gaussian low-pass filter with a standard deviation of 1.5 was considered during the sharpening process.

TABLE I. Description of Classes in Dataset

Class Name	Images	Description
Cell	1,877	Hot spots occuring with square geometry in single cell.
Cell-Multi	1,288	Hot spots occuring with square geometry in multiple cells.
Cracking	941	Module anomaly caused by cracking on module surface.
Hot-Spot	251	Hot spot on a thin film module.
Hot-Spot-Multi	247	Multiple hot spots on a thin film module.
Shadowing	1,056	Sunlight obstructed by vegetation, man-made structures, or adjacent rows.
Diode	1,499	Activated bypass diode, typically 1/3 of module.
Diode-Multi	175	Multiple activated bypass diodes, typically affecting 2/3 of module.
Vegetation	1,639	Panels blocked by vegetation.
Soiling	205	Dirt, dust, or other debris on surface of module.
Offline-Module	828	Entire module is heated.
No-Anomaly	10,000	Nominal solar module.

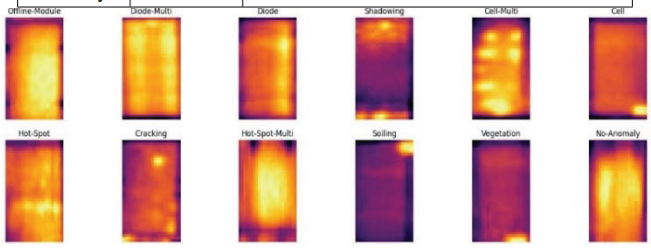

Fig. 3. he sample images obtained from data augmentation

To resolve the ambiguity problem in the data, pictures from the hot spot category were coupled with pictures from the non-hiding category, making a total of 2776 pictures in the dataset.

IV. Deep Learning Models

A. ResNet -50

ResNet-50, a 50-layer network, processes input images with a size of 224×224.Batch normalization and a ReLU activation function come after each convolutional layer. A convolutional layer with a 7×7 kernel size and a stride of 2 is added at the network's startup. After this convolution, there is a max pooling layer with a stride of two, batch normalization, and ReLU activation. The network's building blocks convolutions use 1×1, 3×3, and 1×1 filters. There is a fully linked layer, a SoftMax function, and an average pooling layer at the end of the network is shown in figure 4.

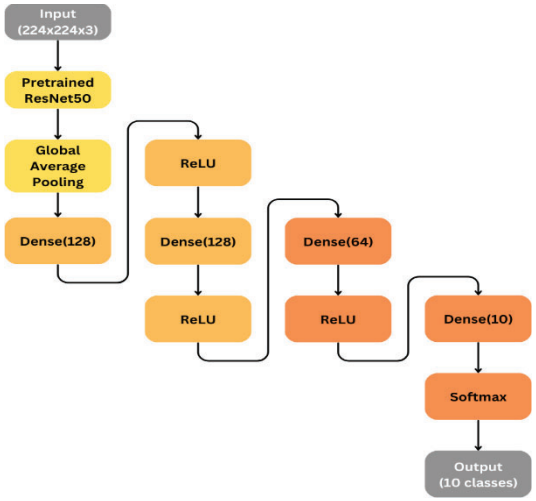

Fig. 4. The general structure of ResNet-50

B. Custom Convolutional Neural Network

Convolutional neural network (CNN) architecture specifically engineered to excel in this specialized task. Unlike generic architectures such as ResNet-50, custom CNN is designed to harness the unique characteristics of infrared data, particularly in identifying hotspot faults [5]. Figure 5. shows the custom CNN architecture. The model employs smaller convolution filters (32 and 64 filters) in the initial layers to capture fine-grained details, such as subtle temperature variations, essential for detecting early-stage hotspots in solar panels. As the network progresses, it employs larger convolution filters (128, 256, and 512 filters) to recognize broader, more complex patterns associated with fully developed faults or anomalies. These deeper layers integrate information from earlier layers, enabling the model to detect higher-level features indicative of significant thermal issues.

Batch normalization is applied after each convolutional layer. This technique normalizes the activations, reducing the internal covariate shift and speeding up convergence during training. The use of maxpooling operations reduces the spatial dimensions of the feature maps, enabling the model to focus on the most critical features. By leveraging domain-specific insights, our custom CNN not only enhances the accuracy of anomaly detection but also improves the model's interpretability and efficiency in processing infrared imagery. This custom architecture highlights our focus on advancing deep learning techniques to tackle complex, real-world challenges efficiently.

Hotspot faults are detected by training this CNN on labeled infrared images that highlight temperature anomalies. The network's filters are designed to capture these subtle temperature differences, which manifest as unique thermal patterns within the infrared spectrum. To further optimize the network, regularization methods such as Dropout are employed in the dense layers, preventing overfitting while enhancing model generalization.

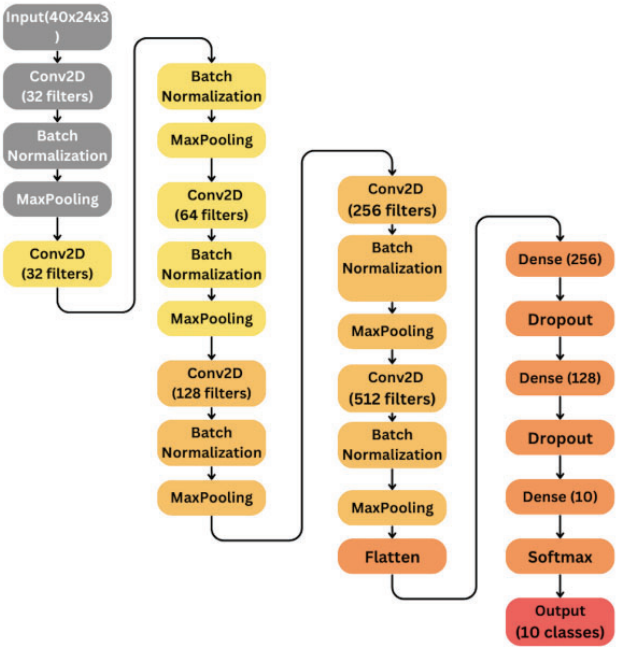

Fig. 5. Customized CNN (Convolutional Neural Network) architecture

Each convolutional layer is followed by Batch Normalization, stabilizing the learning process, and MaxPooling to reduce computational complexity, focusing the network on relevant thermal features.

V. Experimental Studies And Results

The classification of hotspots in solar modules is done by experimental comparison studies. A machine equipped with an AMD Ryzen3 5300U CPU running at 2.60 GHz, Radeon graphics, and 8 GB of RAM is used to run the ResNet50 model. Error minimization is accomplished with a learning rate of 0.001 using the Nadam optimizer. Forty training epochs are used to train the pre-trained deep learning model. Minibatch size is set to 32 during training.

The collected classification results are statistically evaluated, and values for performance metrics like Precision, Recall, Support, and F1-score are computed. Figure 6.a and figure 6 b. shows the training and validation accuracy and loss obtained for Resnet 50.

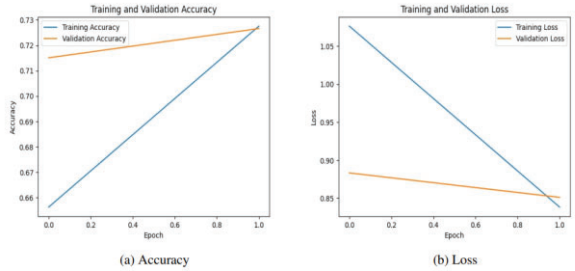

Fig. 6. Plot of Training and Validation of accuracy and loss of ResNet50

Figure 7.a and figure 7 b. shows the training and validation accuracy, and loss obtained for custom CNN.

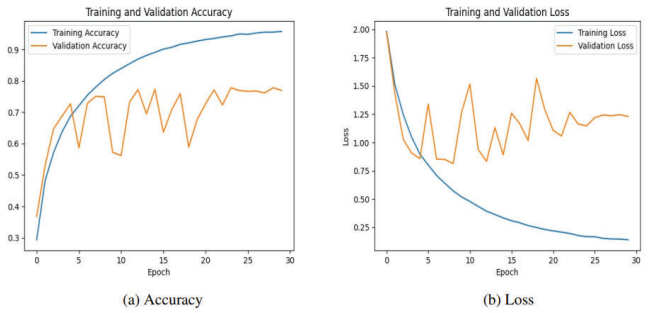

(a) Accuracy (b) Loss

Fig. 7. Plot of Training and Validation of accuracy and loss Custom CNN

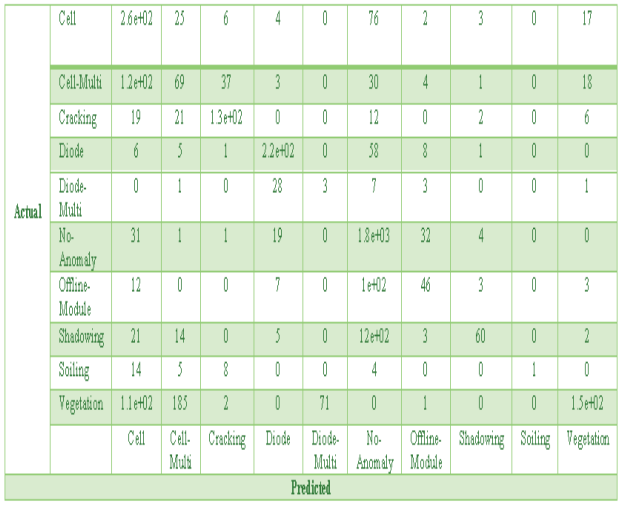

Fig. 8. Confusion Matrix of ResNet50

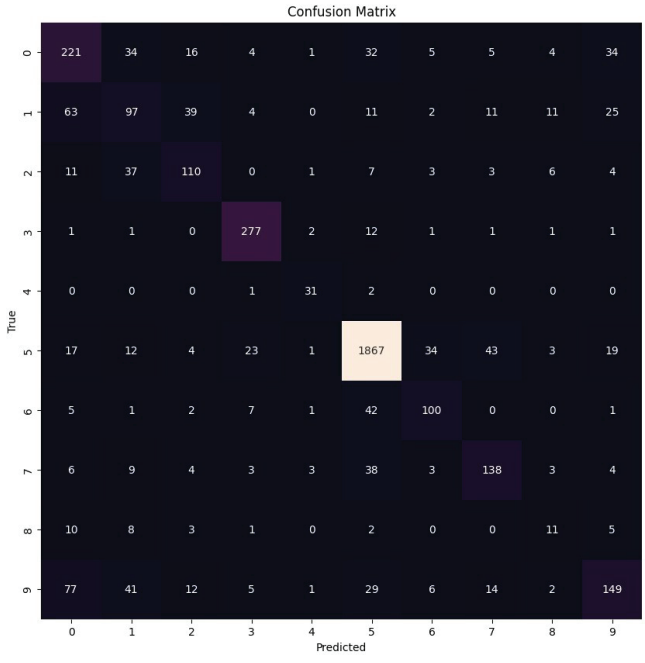

Fig. 9. Confusion Matrix of Custom CNN

Figure 8 and Figure 9 shows the confusion matrix for Resnet 50 and custom CNN architecture.

TABLE II. EXPERIMENT RESULT VALUES OF RESNET50

Classification Report - Resnet-50	Precision	Recall	F1-score	support
Cell	.44	.66	.53	391
Cell-Multi	.44	.24	.31	283
Cracking	.69	.68	.68	186
Diode	.76	.74	.75	300
Diode-Multi	1.00	.07	.13	43
No-Anomaly	.79	.95	.86	1915
Offline-Module	.44	.27	.33	172
Shadowing	.80	.27	.41	220
Soiling	1.00	.03	.06	30
Vegetation	.74	.42	.54	361
Accuracy			.71	3901
Macro Avg	.71	.43	.46	3901
Weighted avg	.71	.71	.68	3901

TABLE III. EXPERIMENT RESULT VALUES OF CUSTOM CNN

Classification Report - Custom CNN	Precision	Recall	F1-score	support
Cell	.54	.62	.58	356
Cell-Multi	.40	.37	.39	263
Cracking	.58	.60	.59	182
Diode	.85	.93	.89	297
Diode-Multi	.76	.91	.83	34
No-Anomaly	.91	.92	.92	2023
Offline-Module	.65	.63	.64	159
Shadowing	.64	.65	.65	211
Soiling	.27	.28	.27	40
Vegetation	.62	.44	.52	336
Accuracy	.77	.77	.77	3901
Macro avg	.62	.64	.63	3901
Weighted avg	.77	.77	.77	3901
Samples avg	.77	.77	.77	3901

Table 2. shows the classification report of ResNet-50 architecture, which focuses on solar anomalies such as Cell, Cracking, Diode, etc., shows varying performance across categories:

- Precision: The Diode-Multi class has the highest precision (1.00), meaning the model made few false positives in this class, but the recall is very low (0.07), indicating many false negatives.
- Recall: The No-Anomaly class has the highest recall (0.95), meaning the model successfully identified most non-anomalous images.
- F1-score: The overall F1-scores indicate moderate performance, with Shadowing having the lowest score (0.41) and the No-Anomaly class having the highest score (0.86).

Table 3. shows the classification report of custom CNN architecture.

- Precision and Recall: The classes vary widely in both precision and recall. Class 4 has the highest precision (0.91) and recall (0.92), indicating excellent performance in this category.

Overall metrics: The macro averages for precision and recall are lower in this report (0.62), while the micro average shows consistent performance (0.77). This suggests the model

performs well on average across all classes but struggles with specific categories.

VI. CONCLUSION

Through meticulous data collection, preprocessing, and model development, we created a robust CNN capable of accurately identifying various anomalies in solar panels such as hotspots, cracks, and other structural defects. Using transfer learning with pre-trained models like ResNet50, we optimized the model's performance and achieved high accuracy in anomaly detection. Our system not only offers near real-time anomaly detection capabilities but also demonstrates reliability and robustness across different environmental conditions and panel configurations. Ultimately, our project contributes to the advancement of sustainable energy practices by improving the performance and safety of solar panels, minimizing downtime, and maximizing energy production.

The above requirements demonstrate the important role of diagnostic equipment in optimizing solar panel performance and lifetime, which is important for supporting the use of renewable energy. These devices detect defects such as temperature and cracks and intervene in a timely manner to improve the overall efficiency, reliability and safety of your solar system. Towards the broad goal of achieving sustainable energy use. When trying to remediate a crime scene, our goal is not only to increase the effectiveness of existing systems, but also to expand their impact across the energy spectrum. This requires constant innovation and renewal to ensure that equipment remains at the forefront of solar energy development and facilitates its integration into renewable energy. While we suppress problems in the panel infrastructure, we are also laying the foundations for a more sustainable and durable energy in the future. This commitment to innovation and development reflects our determination to drive positive change in renewable energy and contribute to the global transition to a cleaner, stronger environment.

REFERENCES

[1] H. Ac¸ıkgo¨z, D. Korkmaz, and C¸. Dandıl, "Classification of Hotspots in Photovoltaic Modules with Deep Learning Methods", TJST, vol. 17, no. 2, pp. 211–221, 2022, doi: 10.55525/tjst.1158854.

[2] Minhhuy Le, Van Su Luong, Dang Khoa Nguyen, Van-Duong Dao, Ngoc Hung Vu, Hong Ha Thi Vu, Remote anomaly detection and classification of solar photovoltaic modules based on deep neural network, Sustainable Energy Technologies and Assessments, Volume 48, 2021, 101545, ISSN 2213-1388, https://doi.org/10.1016/j.seta.2021.101545.

[3] Korkmaz D, Acikgoz H. An efficient fault classification method in solar photovoltaic modules using transfer learning and multi-scale convolu- tional neural network. Eng Appl Artif Intell 2022;113:104959.

[4] Wuqin Tang, Qiang Yang, Kuixiang Xiong, Wenjun Yan, Deep learning based automatic defect identification of photovoltaic module using elec- troluminescence images, Solar Energy, Volume 201, 2020, Pages 453- 460, ISSN 0038-092X, https://doi.org/10.1016/j.solener.2020.03.049.

[5] Deniz Korkmaz and Hakan Acikgoz. An efficient fault classification method in solar photovoltaic modules using transfer learning and multi-scale convolutional neural network. Engineering Applications of Artificial Intelligence, 113:104959, 2022.

[6] Y. Chen, J. Wang, X. Chen, M. Zhu, K. Yang, Z. Wang, and R. Xia, ''Singleimage super-resolution algorithm based on structural self-similarity and deformation block features,'' IEEE Access, vol. 7, pp. 58791–58801, 2019.

[7] T. Peleg and M. Elad, ''A statistical prediction model based on sparse representations for single image super-resolution,'' IEEE Trans. Image Process., vol. 23, no. 6, pp. 2569–2582, Jun. 2014.

[8] K. In Kim and Y. Kwon, ''Single-image super-resolution using sparse regression and natural image prior,'' IEEE Trans. Pattern Anal. Mach. Intell., vol. 32, no. 6, pp. 1127–1133, Jun. 2010

[9] C. Ledig, L. Theis, F. Huszar, J. Caballero, A. Cunningham, A. Acosta, A. Aitken, A. Tejani, J. Totz, Z. Wang, and W. Shi, ''Photo-realistic single image super-resolution using a generative adversarial network,'' in Proc. IEEE Conf. Comput. Vis. Pattern Recognit. (CVPR), Honolulu, HI, USA, Jul. 2017, pp. 105–114.

[10] C. Dong, C. C. Loy, K. He, and X. Tang, ''Image super-resolution using deep convolutional networks,'' IEEE Trans. Pattern Anal. Mach. Intell., vol. 38, no. 2, pp. 295–307, Feb. 2016.